

UC Davis

UC Davis Previously Published Works

Title

Analysis of Lipid Phase Behavior and Protein Conformational Changes in Nanolipoprotein Particles upon Entrapment in Sol-Gel-Derived Silica

Permalink

<https://escholarship.org/uc/item/1xh8v8bm>

Journal

Langmuir, 30(32)

ISSN

0743-7463

Authors

Zeno, Wade F
Hilt, Silvia
Aravagiri, Kannan K
[et al.](#)

Publication Date

2014-08-19

DOI

10.1021/la5025058

Peer reviewed

This document is confidential and is proprietary to the American Chemical Society and its authors. Do not copy or disclose without written permission. If you have received this item in error, notify the sender and delete all copies.

ANALYSIS OF LIPID PHASE BEHAVIOR AND PROTEIN CONFORMATIONAL CHANGES IN NANOLIPOPROTEIN PARTICLES UPON ENTRAPMENT IN SOL-GEL DERIVED SILICA

Journal:	<i>Langmuir</i>
Manuscript ID:	la-2014-025058.R1
Manuscript Type:	Article
Date Submitted by the Author:	n/a
Complete List of Authors:	Zeno, Wade; University of California, Davis, Chemical Engineering and Materials Science Hilt, Silvia; University of California, Davis, Molecular and Cellular Biology Aravagiri, Kannan; University of California, Davis, Chemical Engineering and Materials Science Risbud, Subhash; UC Davis, Materials Science Voss, John; University of California Davis, Biological Chemistry Parikh, Atul; University of California, Davis, Department of Applied Science Longo, Marjorie; University of California, Davis, Chemical Engineering and Materials Science

SCHOLARONE™
Manuscripts

1
2
3 ANALYSIS OF LIPID PHASE BEHAVIOR AND PROTEIN CONFORMATIONAL
4
5 CHANGES IN NANOLIPOPROTEIN PARTICLES UPON ENTRAPMENT IN SOL-GEL
6
7
8 DERIVED SILICA
9

10 Wade F. Zeno[‡], Silvia Hilt[¶], Kannan K. Aravagiri[‡], Subhash H. Risbud[‡], John C. Voss[¶], Atul N.
11 Parikh[‡], and Marjorie L. Longo^{*‡}
12
13

14
15 [‡]Department of Chemical Engineering and Materials Science / [¶]Department of Biochemistry and
16
17 Molecular Medicine, University of California Davis, Davis, California, 95616
18
19

20 **ABSTRACT**
21

22 The entrapment of Nanolipoprotein Particles (NLPs) and liposomes in transparent, nanoporous
23
24 silica gel derived from the precursor Tetramethylorthosilicate (TMOS) was investigated. NLPs
25
26 are discoidal patches of lipid bilayer that are belted by amphiphilic scaffold proteins and have an
27
28 average thickness of 5 nm. The NLPs in this work had a diameter of roughly 15 nm and utilized
29
30 Membrane Scaffold Protein (MSP), a genetically altered variant of Apolipoprotein A-I.
31
32 Liposomes have previously been examined inside of silica sol-gels and have been shown to
33
34 exhibit instability. This is attributed to their size (~150 nm) and altered structure and constrained
35
36 lipid dynamics upon entrapment within the nanometer scale pores (5-50 nm) of the silica gel. By
37
38 contrast, the dimensional match of NLPs with the intrinsic pore sizes of silica gel opens the
39
40 possibility for their entrapment without disruption. Here we demonstrate that NLPs are more
41
42 compatible with the nanometer scale size of the porous environment by analysis of lipid phase
43
44 behavior via fluorescence anisotropy and analysis of scaffold protein secondary structure via
45
46 circular dichroism spectroscopy. Our results showed that the lipid phase behavior of NLPs
47
48 entrapped inside of silica gel display closer resemblance to its solution behavior, more so than
49
50 liposomes, and that the MSP in the NLPs maintain the high degree of alpha-helix secondary
51
52
53
54
55
56
57
58
59
60

1
2
3 structure associated with functional protein-lipid interactions after entrapment. We also
4
5 examined the effects of residual methanol on lipid phase behavior and size of NLPs and found
6
7 that it exerts different influences in solution and in silica gel; unlike in free solution, silica
8
9 entrapment may be inhibiting NLP size increase and/or aggregation. These findings set
10
11 precedence for a bio-inorganic hybrid nanomaterial that could incorporate functional integral
12
13 membrane proteins.
14
15

16 17 **INTRODUCTION**

18
19 Over the past several decades, the entrapment of proteins in transparent, mesoporous silica has
20
21 been of significant interest to scientists and engineers spanning a broad spectrum of disciplines.¹⁻
22
23 ³ In more recent history, integral membrane proteins (IMPs) have been of particular interest for
24
25 sol-gel derived silica entrapment due to their differing functionalities that can be exploited to
26
27 tailor these systems for accommodating various applications such as biosensing, affinity
28
29 chromatography, high-throughput drug screening, and bio-reaction engineering.⁴⁻⁷ IMPs contain
30
31 both hydrophobic and hydrophilic amino acid residues, thus they are either partially or
32
33 completely embedded within amphiphilic lipid bilayers of cell membranes. This allows the IMPs
34
35 to maintain their proper tertiary conformation. The necessity of lipid bilayers for proper IMP
36
37 functionality requires an entrapment system that minimally modulates the physical and structural
38
39 properties of the lipid bilayers; direct modification of the lipid bilayer structures would adversely
40
41 affect protein conformation within it.⁸⁻¹¹ Therefore, the investigation of the stability of lipid
42
43 bilayer derived structures (i.e. nanolipoprotein particles and liposomes) entrapped within silica
44
45 gel is essential to the development of viable, efficient IMP derived bio-inorganic hybrid
46
47 materials.
48
49
50
51
52
53
54
55
56
57
58
59
60

1
2
3 During the 1990s, research groups of Bright, Friedman, Kostic, and Brennan examined the
4 properties of various water-soluble proteins entrapped in silica gels derived from alkoxy silane
5 precursors.¹²⁻¹⁵ Their work spurred the development of optimized, biocompatible techniques for
6 a variety of water-soluble proteins. These techniques would later be applied towards liposome
7 entrapment. One of the main techniques included the addition of glycerol and osmolytes, such as
8 sugar, to alter protein hydration.¹⁶⁻¹⁷ However, this approach did not address the problematic
9 presence of high concentrations of alcohol that resulted from the hydrolysis reactions of
10 alkoxy silane precursors. The presence of alcohols is especially detrimental to lipid bilayers, as
11 sufficiently high concentrations will lead to alcohol significantly partitioning into the bilayer,
12 causing it to interdigitate.¹⁸ To address this, Brennan's group further pioneered the development
13 of biocompatible sol-gel chemistries that consisted of modified alkoxy silane precursors bearing
14 covalently attached sugar moieties and/or glycerol.¹⁹⁻²⁰ Depending on the specific precursor, the
15 quantity of alcohol liberated during hydrolysis reactions was either greatly reduced or completely
16 removed and the additives were unable to leach from the gel.
17
18
19
20
21
22
23
24
25
26
27
28
29
30
31
32
33
34
35

36 In 2002, Besanger *et al.* examined the stability of 1,2-dipalmitoyl-*sn*-glycero-3-
37 phosphatidylcholine (DPPC) liposomes within silica gels derived from three different precursors:
38 an unmodified alkoxy silane (tetraethylorthosilicate or TEOS), an alkoxy silane with covalently
39 attached glycerol (diglyceryl silane or DGS), and sodium silicate (SS).²¹ Their work
40 demonstrated that the use of DGS- and SS-derived gels permitted the DPPC liposomes to exhibit
41 phase transitions as they would in solution, while the use of TEOS derived gels did not. Also,
42 they depicted, via confocal fluorescence imaging, that the liposomes are capable of undergoing a
43 variety of conformational changes once trapped inside of the gel, forming aggregates or bicelles.
44
45
46
47
48
49
50
51
52
53
54
55
56
57
58
59
60
61
62
63
64
65
66
67
68
69
70
71
72
73
74
75
76
77
78
79
80
81
82
83
84
85
86
87
88
89
90
91
92
93
94
95
96
97
98
99
100

Though the DGS- and SS-derived silica gels seemed to work favorably at first, the DPPC

1
2
3 liposomes eventually lost the ability to undergo phase transitions several days later. It was
4
5 speculated that this was due to rupturing of the liposomes. Halder *et al.* would corroborate this
6
7 theory in 2004 by examining the solvation dynamics of coumarin 480 inside of liposomes
8
9 entrapped in silica gel.²² Other analysis of liposome-silica interactions have elucidated that silica
10
11 has a propensity for deforming liposomes, causing them to rupture and fuse to the surface.²³
12
13 Moreover, silica is actually a very common substrate for performing liposomal fusion to make
14
15 supported lipid bilayers.²⁴⁻²⁶
16
17

18
19 An alternate approach for circumventing the problematic alcohol presence was presented in
20
21 2002 by Ferrer *et al.* It consisted of a simple technique where rotary evaporation was used prior
22
23 to incorporation of biological species.²⁷ This approach was later utilized by Luo *et al.* 2005 to
24
25 entrap liposomes bearing the IMPs bacteriorhodopsin and ATP-synthase in silica gels derived
26
27 from the precursor tetramethylorthosilicate (TMOS).²⁸ Though protein activity was observed
28
29 after entrapment, the condition of the liposomal hosts was not examined. Based on their analysis,
30
31 it is unknown whether or not the protein was functioning near its optimal activity, the liposomes
32
33 retained their structure over time, or if this approach would work well for other biologically
34
35 significant IMPs.
36
37

38
39 From these previous works, it can be seen that liposomes undergo structural changes and
40
41 altered lipid dynamics upon entrapment, thus they are not optimal biological membrane hosts for
42
43 IMPs inside of silica gel. In addition, the size mismatch of liposomes (~100-200 nm in solution)
44
45 with mesoporous silica (5-50 nm pores) is a limiting factor in their successful implementation as
46
47 biological membrane host for IMPs.²⁹ Here we look to improve upon the use of liposomes in
48
49 silica gel by instead utilizing nanolipoprotein particles (NLPs) as biological membrane hosts.
50
51 NLPs are discoidal patches of lipid bilayer associated with amphiphilic scaffold proteins that
52
53
54
55
56
57
58
59
60

1
2
3 interact with the hydrophobic domain of the bilayer by wrapping around the particle periphery,
4 making the entire structure water soluble. NLPs have an average thickness of 5 nm, with a
5 diameter ranging from 10-25 nm depending on the stoichiometric ratios and types of lipids and
6 scaffold proteins being used.³⁰ This allows NLPs to be more compatible with the pore size (5-50
7 nm) of mesoporous silica and bear more resemblance to water-soluble proteins - the molecules
8 for which this architecture was optimized - than liposomes. Therefore, here we perform
9 entrapment of NLPs using a quick, simple sol-gel processing technique for TMOS that includes
10 evaporation of the majority of the methanol after the hydrolysis reactions. The lipid phase
11 behavior of entrapped NLPs in comparison to entrapped liposomes was observed using
12 fluorescence anisotropy measurements, while the secondary structure of the scaffold protein was
13 examined via circular dichroism spectroscopy. We found that liposomes exhibited more
14 significant modulations in their phase behavior upon entrapment in silica gel than NLPs and that
15 modulations caused by residual methanol for both liposomes and NLPs are relatively small.
16 Also, the scaffold protein of NLPs maintained a conformation indicative of protein-lipid
17 interactions, thus strongly suggesting that there were minimal alterations in structure for NLPs.
18 Our results demonstrate that NLPs are more favorable for silica gel entrapment than liposomes.
19
20
21
22
23
24
25
26
27
28
29
30
31
32
33
34
35
36
37
38
39
40
41

42 MATERIALS AND METHODS

43
44 **Materials.** MSP is a His-tagged Membrane Scaffold Protein (MSP1E3D1, Sigma-Aldrich, Inc),
45 which is comprised of residues 56-243 of human apoA-I and a 22 amino acid N-terminal fusion
46 containing the His tag, a spacer sequence, and the TEV protease site. Imidazole ($\geq 99\%$),
47 Tetramethyl Orthosilicate (TMOS) ($\geq 99\%$), 1,6-Diphenyl-1,3,5-hexatriene (DPH) ($\geq 98\%$),
48 Ethanol (200 Proof), Sodium Chloride ($\geq 99\%$), Methanol ($\geq 99\%$), and Sodium Cholate (\geq
49 99%) were also purchased from Sigma-Aldrich, Inc. 1,2-dipentadecanoyl-sn-glycero-3-
50
51
52
53
54
55
56
57
58
59
60

1
2
3 phosphocholine (Di15:0PC) was purchased in chloroform (10 mg/mL concentration) from
4
5 Avanti Polar Lipids, Inc. Ni-NTA agarose was purchased from 5 PRIME, Inc. The
6
7 Tris(hydroxymethyl)aminomethane (MB Grade) and Hydrochloric Acid (12.1 N) used to prepare
8
9 a Tris-HCl buffer stock solution (500 mM, pH 7.5) were purchased from USB Corporation and
10
11 Fisher Scientific International, Inc., respectively. All water used in these experiments was
12
13 purified in a Barnstead Nanopure System (Barnstead Thermolyne, Dubuque, IA) with a
14
15 resistivity $\geq 17.9 \text{ M}\Omega\cdot\text{cm}$.
16
17
18

19
20 **Preparation of Di15:0PC Liposomes.** For a single preparation, an appropriate aliquot of
21
22 Di15:0PC was removed from the 10 mg/ml chloroform stock solution, placed into a glass conical
23
24 vial, dried with nitrogen, and then placed under mild vacuum for at least 4 hours to fully
25
26 evaporate all of the chloroform. The lipid film was then rehydrated with a reconstitution buffer
27
28 (20 mM Tris, 100 mM NaCl, pH 7.4) to a final lipid concentration of 2 mg/mL and heated to
29
30 80°C for at least 5 minutes. After hydration and heating, the lipids were extruded through 100
31
32 nm pore membranes in an extruder (Avestin, Inc. Ottawa, Canada). Finally, a small fraction of
33
34 the resulting liposome solution was used for size determination via a Particle Size Analyzer
35
36 (Brookhaven Instruments Corporation, Holtsville, NY).
37
38
39

40
41 **Preparation of Di15:0PC MSP NLPs.** NLP batches were synthesized by first placing a
42
43 stoichiometric excess (6 mg) of Di15:0PC in chloroform solution inside of a glass conical vial.
44
45 The contents were first dried using nitrogen, and then placed under mild vacuum for at least 4
46
47 hours. Afterward, the dried lipid film was rehydrated and solubilized with a Sodium Cholate
48
49 Reconstitution Buffer (40 mM sodium cholate, 20 mM Tris, 100 mM NaCl) and transferred to a
50
51 plastic centrifuge tube, where it was allowed to further mix at room temperature ($22 \pm 1^\circ\text{C}$) on a
52
53 vortex mixer (Fischer Scientific Hampton, New Hampshire) for 30 minutes. Next, 0.93 mg of
54
55
56
57
58
59
60

1
2
3 His-Tagged MSP was added to the centrifuge tube and allowed to incubate at room temperature
4 and 300 RPM for 1 hour. After incubation, the NLP reaction mixture was transferred to a 10,000
5 MWCO dialysis filter (Thermo Scientific, Rockford, IL) and dialyzed against a Reconstitution
6 Buffer (20 mM Tris, 100 mM NaCl) at 250X volume excess to remove cholate. Dialysis was
7 performed for 4 hours at room temperature and 20 additional hours at 4°C. Over the course of the
8 24 hour dialysis, the buffer was exchanged three times (250⁴ overall cholate dilution factor).
9 After dialysis, the NLPs were purified using Ni-NTA agarose. The solution of His-Tagged NLPs
10 was incubated with Ni-NTA agarose at 4°C for at least 2 hours. The ratio of NLPs and Ni-NTA
11 agarose was prepared such that the concentration of NLPs was far below the maximum binding
12 capacity of the Ni-NTA agarose. After incubation, the agarose was separated via gentle
13 centrifugation (500 RPM) and the supernatant aqueous phase was removed. Centrifugation was
14 also used during the subsequent wash and elution steps to separate the agarose from the aqueous
15 phase. The agarose was washed 4 times with a Wash Buffer (20 mM imidazole, 20 mM Tris, 100
16 mM NaCl). The agarose was then eluted 4 times with an Elution Buffer (400 mM imidazole, 20
17 mM Tris, 100 mM NaCl). The supernatant liquid removed after each elution was concentrated
18 using 100,000 MWCO centrifugal concentrators (Vivaproducts, Inc. Littleton, MA) and
19 combined for a total volume of roughly 1 mL. NLPs were then dialyzed again under the same
20 conditions previously mentioned for the purpose of imidazole removal. The concentration of
21 MSP was determined using a UV-Vis spectrophotometer (Shimadzu Scientific Instruments,
22 Columbia, MD) to measure the concentration of MSP via absorbance at 280 nm. The lipid
23 concentration was determined by synthesizing a separate batch of NLPs using Di15:0PC that was
24 laced with a trace amount of fluorescent Oregon Green® 488 DHPE (Life Technologies,
25 Carlsbad, CA) and using an Oregon Green standard curve to measure fluorescence intensities of
26
27
28
29
30
31
32
33
34
35
36
37
38
39
40
41
42
43
44
45
46
47
48
49
50
51
52
53
54
55
56
57
58
59
60

1
2
3 the resulting NLP batch with a fluorescence spectrophotometer (PerkinElmer, Inc., Waltham,
4 MA). The lipid to protein ratio (4mg:1mg) was consistent with the expected ratio of MSPs to
5 lipids (2:375).³⁰ The size of the NLPs was measured using a particle size analyzer (Brookhaven
6 Instruments Corporation, Holtsville, NY). The acquired Stokes diameter was converted to a
7 discoidal diameter using known thicknesses of phosphatidylcholine bilayers (See Supporting
8 Information).

9
10
11
12
13
14
15
16
17 **Entrapment of Liposomes and NLPs in Silica Gel.** For a typical preparation, 5.6 mL of 0.01 M
18 HCl in nanopure water was combined with 7.6 mL of TMOS in a round bottom flask and swirled
19 until a uniform, cloudy phase was observed. The solution was then subjected to sonication in a
20 bath sonicator for 10 minutes, followed by rotary evaporation (340 mbar reduced pressure, 50°C)
21 for 20 minutes to promote rapid removal of methanol liberated during the hydrolysis reactions.
22 The solution was then passed through a 0.45 μ m filter, resulting in roughly 4 mL of a clear silica
23 sol. Of the 4 mL of silica sol, 1 mL was placed into a methacrylate cuvette, followed by 1 mL of
24 a stronger Reconstitution Buffer (34 mM Tris, 100 mM NaCl) in order to neutralize the pH.
25 Afterward, 1 mL of either a 20X diluted liposome solution or 20X diluted NLP solution in
26 regular Reconstitution Buffer (20 mM Tris, 100 mM NaCl) was added to the methacrylate
27 cuvette. The liposome stock solution was typically 2.8 mM 15:0 PC (final concentration 56 μ M
28 inside gel), while the NLP stock solution was typically 20 μ M MSP (final concentration 400 nM
29 inside gel). Gelation typically occurred within 2 minutes after addition of the liposomes or NLPs.
30
31
32
33
34
35
36
37
38
39
40
41
42
43
44
45
46
47
48

49 **Fluorescence Anisotropy Measurements.** 10 μ L of a 100 μ M DPH stock solution in ethanol
50 was added to either liposome or NLP solutions in 1 mL volumes of Reconstitution Buffer (20
51 mM Tris, 100 mM NaCl). Afterward, these samples were either diluted further (3X) and used for
52 solution anisotropy readings, or added as the final 1 mL aliquot during the aforementioned
53
54
55
56
57
58
59
60

1
2
3 entrapment/gelation process and used for gel anisotropy readings. Anisotropy values (r) are
4 determined by the difference in polarized light intensity emitted parallel and perpendicular to the
5 excitation source normalized by the total light intensity emitted, as shown in Equation 1.³¹
6
7
8
9

$$10 \quad r = \frac{I_{\parallel} - I_{\perp}}{I_{\parallel} + 2I_{\perp}} \quad (1)$$

11
12
13 The measurements were carried out on a Perkin Elmer LS 55 Fluorescence Spectrometer
14 equipped with a PTP-1 Fluorescence Peltier System (PerkinElmer, Inc., Waltham, MA). A
15 wavelength of 360 nm was used for excitation, while emission intensities at 440 nm were used
16 for determining anisotropy values. Band passes of 3 nm and 5 nm were used on the excitation
17 and emission monochromators, respectively. The anisotropy values were recorded at varying
18 temperature intervals ($\leq 4^{\circ}\text{C}$) as temperature was raised at an average rate of 0.4 $^{\circ}\text{C}/\text{minute}$.
19
20
21
22
23
24
25
26
27
28
29
30
31
32
33
34
35
36
37
38
39
40
41
42
43
44
45
46
47
48
49
50
51
52
53
54
55
56
57
58
59
60

Cooperativity and Melting Temperature Determination. The anisotropy vs. temperature
experimental data was regressed using the method of least squares for an empirical phase
transition model shown in Equation 2, where the parameters, r_{\max} , r_{\min} , T_m , and n are maximum
anisotropy, minimum anisotropy, melting temperature, and cooperativity index, respectively.³²

$$r(T) = \frac{r_{\max} - r_{\min}}{1 + e^{(T - T_m)n}} + r_{\min} + AT + BT^2 \quad (2)$$

A and B are constant coefficients for the quadratic baseline. Ignoring the quadratic baseline,
Equation 2 depicts a sigmoid function with asymptotic end behavior in the limit as T is

1
2
3 significantly far from the phase transition region. The parameters r_{\max} and r_{\min} represent the
4 vertical displacement of the plot, while T_m corresponds to the inflection point (for significantly
5 small values of B) and n corresponds to the broadness of the phase transition region. A quadratic
6 baseline can be used in the vicinity of the phase transition region to more accurately capture the
7 manner in which anisotropy varies with temperature, as well as any asymmetry about the
8 inflection point. The parameters A and B were chosen to be the average of all of the individually
9 regressed data plots. This was due to a trade-off between “n” and the quadratic baseline during
10 the regression process; “A and B” can influence the value of “n”. By fixing “A and B”, the
11 change in “n” between different plots is almost entirely attributed to the sample, with minimal
12 effect from other parameters. To implement this, each plot was regressed individually while its
13 values for A and B were recorded. Once all of the values were recorded and averaged, all of the
14 plots were re-regressed with fixed values for A and B (See Supporting Information). These
15 values were the overall average from the previous regressions.

16
17
18
19
20
21
22
23
24
25
26
27
28
29
30
31
32
33
34
35 **Circular Dichroism Spectroscopy of NLPs.** In order to perform circular dichroism (CD)
36 spectroscopy, the 20 mM Tris 100 mM NaCl buffer was replaced with a 25 mM Phosphate 100
37 mM NaF buffer due to absorbance of Tris and chloride in the UV region of interest. Solution and
38 gelated measurements were performed on a Jasco J-715 spectropolarimeter with a 2 cm/min scan
39 speed (JASCO Easton, MD). Data points were collected as averages of 3 scans from 260 to
40 190nm, at room temperature in a demountable close-ended far UV (Q) 1mm path length quartz
41 cuvette cell type 20C (STARNA Cells) for the silica gel samples and in a 1mm path length open
42 end quartz cuvette for the solution samples. The final concentrations of MSP were 20 μM in
43 solution and 60 μM in silica gel.
44
45
46
47
48
49
50
51
52
53
54
55
56
57
58
59
60

1
2
3 **Estimation of Alpha-Helix Content from CD Spectra.** The alpha-helical content was
4 determined by first converting the measured ellipticity at 222 nm to a molar ellipticity using
5 Equation 3, where $[\theta]_{\text{molar}}$, MRW, θ_{222} , l , and c are the molar ellipticity ($\text{deg cm}^2 \text{ dmol}^{-1}$), MSP
6 mean residue weight (g/mol), ellipticity (degrees), cuvette path length (cm), and MSP
7 concentration (g/mL), respectively.
8
9

$$[\theta]_{\text{molar}} = (\text{MRW})(\theta_{222})/(10lc) \quad (3)$$

10
11
12
13
14
15
16
17
18
19
20
21
22
23
24
25
26
27
28
29
30
31
32
33
34
35
36
37
38
39
40
41
42
43
44
45
46
47
48
49
50
51
52
53
54
55
56
57
58
59
60
Once this was obtained, a common correlation³³ shown in Equation 4 was used to estimate the
percentage of alpha-helical content.

$$\% \text{ alpha - helix} = (-[\theta]_{\text{molar}} + 3000)/39000 \quad (4)$$

RESULTS

29
30
31
32
33
34
35
36
37
38
39
40
41
42
43
44
45
46
47
48
49
50
51
52
53
54
55
56
57
58
59
60
Fluorescence Anisotropy Measurements and Regressions. Fluorescence anisotropy of the
membrane-inserting probe 1,6-diphenyl-1,3,5-hexatriene (DPH) was used to investigate the
phase behavior of Di15:0PC carbonyl tails within liposomes and NLPs. Di15:0PC was used
instead of other biologically prevalent PC lipids (such as DMPC or DPPC) due to the
compatibility of its phase transition temperature with the heating/cooling speeds of the Peltier
element in the experimental set up, which allowed for higher throughput of samples in a given
period of time (See Supporting Information). Liposomes had a Stokes diameter of 166.5 ± 1.8
nm, while NLPs had a Stokes diameter of 11.7 ± 2.2 nm and corresponding discoidal diameter of
 14.8 ± 4.4 nm by dynamic light scattering. We obtained fluorescence anisotropy values using
equation 1 at a range of temperatures that included the main phase transition and in two
environments - aqueous buffer solution and porous silica gel derived from the alkoxy silane
precursor, tetramethylorthosilicate (TMOS). As shown in Fig. 1A, the phase transition from a

1
2
3 solid lipid phase to a liquid disordered lipid phase, observed as a decrease in anisotropy with
4 increasing temperature, was broader for NLPs than that of the liposomes in buffer.
5
6

7
8 This corresponds to the disparity in the cooperativity indices (n) of the phase transition,
9 obtained by fitting to equation 2. When lipid bilayers undergo a phase transition, the transition
10 occurs involving multiple subunits known as cooperative units. The cooperativity index is a
11 relative scale that is directly proportional to the size of the cooperative unit. The NLPs have an
12 average index of 0.36 ± 0.20 and the liposomes have an average index of 1.79 ± 0.24 , both in
13 solution. Fig. 1A also illustrates the shift in the midpoint of the phase transition (T_m) to higher
14 temperature for NLPs in comparison to liposomes. By fitting this data to equation 2, T_m values
15 are found to be 35.1 ± 0.1 °C and 37.7 ± 0.6 °C on average for the liposomes and NLPs,
16 respectively. Immediately after entrapment in silica gel (day 1), phase transitions can be
17 observed by the decrease in anisotropy with increasing temperature as shown in Fig. 1B.
18
19 However the anisotropy range – the overall ordinate axis difference between the maximum and
20 minimum anisotropy values – was reduced for both NLPs and liposomes in comparison to
21 solution anisotropy ranges. In addition, Fig. 1 and Table 1 show that the T_m values of both NLPs
22 and liposomes entrapped in silica gel are elevated compared to their solution values.
23
24
25
26
27
28
29
30
31
32
33
34
35
36
37
38
39
40
41
42
43
44
45
46
47
48
49
50
51
52
53
54
55
56
57
58
59
60

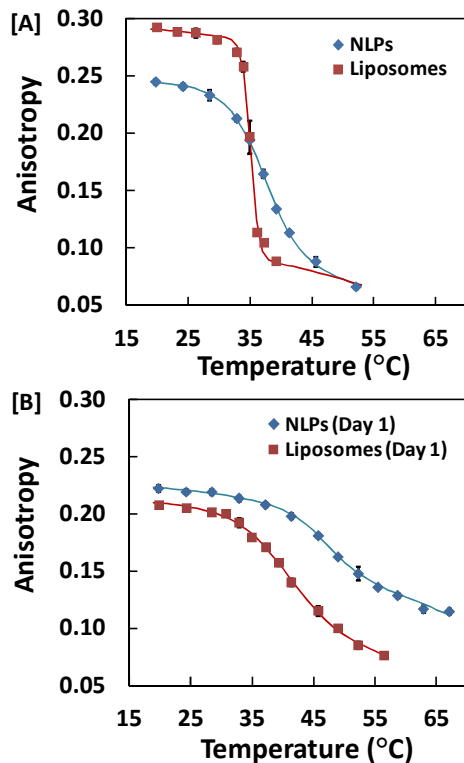


Figure 1: The measured anisotropy values of NLPs and Liposomes in [A] 20 mM Tris 100 nM NaCl buffer and [B] silica gel after initial entrapment, with corresponding regression curves as temperature was increased.

Table 1 illustrates that the cooperativity indices for NLPs and liposomes entrapped within silica gel were on the same order of magnitude, with the NLP values being slightly higher. These values were on the same order of magnitude of NLP cooperativity in solution, but were an order of magnitude lower than that of liposome cooperativity in solution. This is depicted in Fig. 2A where the cooperativity of NLPs and liposomes entrapped in silica gel are plotted over a 5-6 week period, normalized by their respective solution values.

Table 1: Selected regression parameters for liposomes and NLPs in various conditions

	Condition	$T_m(^{\circ}\text{C})$	n	$n_{\text{normalized}}$
NLPs	Solution	37.7 ± 0.2	0.36 ± 0.03	1
	Gel (No Rotovap, Day 1)	40.0 ± 0.5	0.35 ± 0.05	0.98 ± 0.15
	Gel (Day 1)	46.3 ± 0.6	0.33 ± 0.06	0.93 ± 0.10
	Gel (Day 7)	47.9 ± 0.7	0.30 ± 0.05	0.85 ± 0.12
	Gel (Day 14)	48.2 ± 0.4	0.25 ± 0.02	0.72 ± 0.07
	Gel (Day 36)	49.5 ± 0.8	0.25 ± 0.05	0.72 ± 0.14
Liposomes	Solution	35.1 ± 0.1	1.79 ± 0.30	1
	Gel (Day 1)	41.3 ± 0.8	0.22 ± 0.03	0.12 ± 0.03
	Gel (Day 7)	42.1 ± 0.6	0.26 ± 0.02	0.13 ± 0.02
	Gel (Day 13)	41.8 ± 0.5	0.28 ± 0.03	0.14 ± 0.02
	Gel (Day 39)	40.4 ± 0.9	0.22 ± 0.03	0.14 ± 0.03

The normalized cooperativity for NLPs started near unity and decayed to a constant value of approximately 0.7 over the course of 2 weeks (Fig. 2A). The liposomes maintained a constant normalized cooperativity between 0.1 and 0.2 over the entire 5-6 week period (Fig 2A). In solution, cooperativity didn't exhibit any significant changes over time for both NLPs and liposomes as it remained unaffected over the course of 3 weeks (See Table S1 and Table S2). In addition to the normalized cooperativity, the phase transition temperature (T_m) of liposomes entrapped within silica gel remained relatively constant in the 40-42 $^{\circ}\text{C}$ region over the course of the 5-6 week period, as shown in Fig. 2B. The NLP T_m was higher, as it gradually increased and leveled off in the 46-50 $^{\circ}\text{C}$ region as shown in Fig. 2B. As with cooperativity, T_m also remained relatively unaffected in solution over the course of 3 weeks for both NLPs and liposomes (See Table S1 and S2). For all samples, the observed anisotropy curves were reversible with respect to temperature in solution. However, they were not reversible in silica gel and appeared somewhat broadened (data not shown). Therefore, different samples were independently aged and used to generate single sets of parameters. The plots in Fig. 2 are the averaged scatter plots of the regressed values for 20 silica gels entrapping NLPs and 9 silica gels entrapping liposomes.

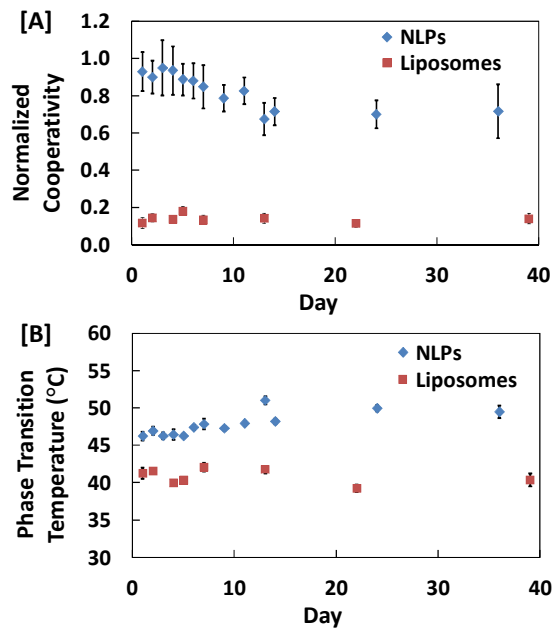


Figure 2: The regressed values for [A] cooperativity and [B] phase transition temperature of NLP and liposome samples entrapped in silica gel over the course of 5-6 weeks.

Upon synthesis of TMOS derived silica gel, methanol was liberated and reduced using rotary evaporation. The methanol content in rotary evaporated silica was determined to be roughly 5 v/v%, while untreated silica had a methanol concentration of 24 v/v% (See Supporting Information). Due its presence, the effect of methanol on the phase behavior of Di15:0PC in NLPs and liposomes was examined. As shown in Fig. 3, the anisotropy values of NLPs in buffer solution decreased in nearly constant intervals as the concentration of methanol was increased at all temperatures. This was also observed for liposomes (See Fig. S3).

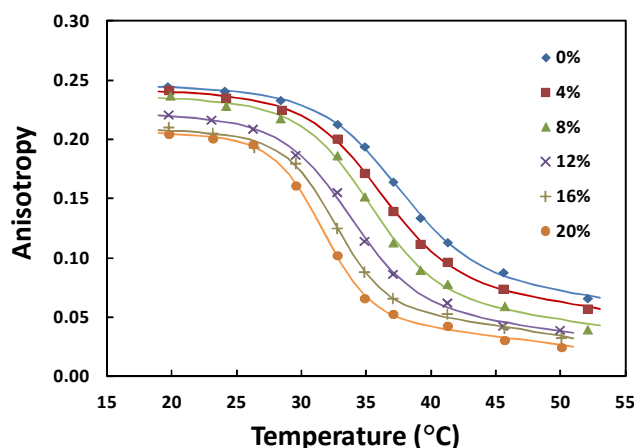
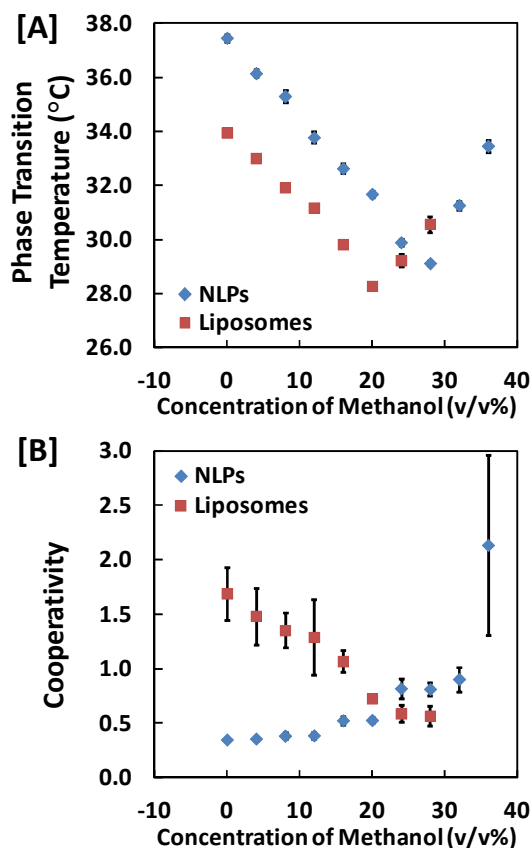


Figure 3: The measured anisotropy values and corresponding regression curves of different NLP samples in 20 mM Tris 100 mM NaCl at various concentrations of methanol (v/v%).

Moreover, the T_m values for NLPs and liposomes monotonically decreased and then increased with increasing methanol concentration, as shown in Fig. 4A, with minimum T_m values of 29.1 ± 0.1 °C at 28 ± 4 v/v% methanol and 28.3 ± 0.1 °C at 20 ± 4 v/v% methanol, respectively. Cooperativity indices, obtained by fits to equation 2, did not show corresponding minima or maxima and instead increased for NLPs and decreased for liposomes with increasing methanol concentration as shown in Fig. 4B

As the methanol concentration was increased in solution, the size of particles in NLP samples also increased. At 0, 15, and 30 v/v%, the Stokes diameter of particles in NLP solution samples was 11.7 ± 2.2 , 17.3 ± 3.2 , and 93.0 ± 3.5 nm, respectively (see Table S3). The effect of methanol was also examined inside silica gel for NLPs, where samples without rotary evaporation during the sol-gel processing were compared to samples utilizing it. In Fig. 5 and Table 1, it is shown that elimination of the rotary evaporation step, which corresponds to higher methanol concentrations, resulted in lowered anisotropy values and a reduced phase transition temperature (46.3 ± 0.6 °C for rotary evaporated samples and 40.0 ± 0.5 °C for non-rotary

1
2
3 evaporated samples). In addition, it was observed that the cooperativity change was small (0.33
4
5 ± 0.06 °C for rotary evaporated samples and 0.35 ± 0.05 °C for non-rotary evaporated samples).
6
7



37 Figure 4: The regressed parameters for [A] phase transition temperature (T_m) and [B]
38 cooperativity (n) of NLPs and liposomes in 20 mM Tris 100 mM NaCl buffer in methanol-
39 aqueous buffer solutions.
40
41
42
43
44

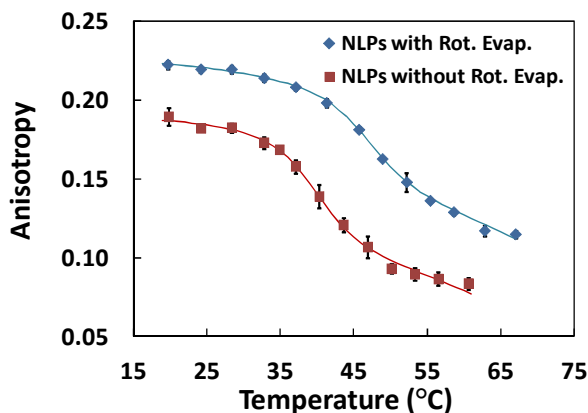


Figure 5: The measured anisotropy values of NLPs in silica gel after initial entrapment with and without the use of rotary evaporation during the sol-gel processing.

Circular Dichroism Spectra. Far-UV circular dichroism spectroscopy was used to examine the secondary structures of the scaffold protein MSP in lipid-free and lipid bound conformations. Fig. 6 shows spectra in terms of ellipticity vs. wavelength for MSP alone (lipid-free) and MSP assembled in NLPs (lipid-bound) in both solution and gel-entrapped states. It can be seen that there were vertical shifts in spectral intensity for MSP over the course of a week. These shifts were more prominent for samples where MSP was in a lipid-free conformation (Fig. 6A and Fig. 6D) in comparison to samples where it was in a lipid-bound conformation (Fig. 6B and Fig. 6E) in both solution and silica gel, respectively.

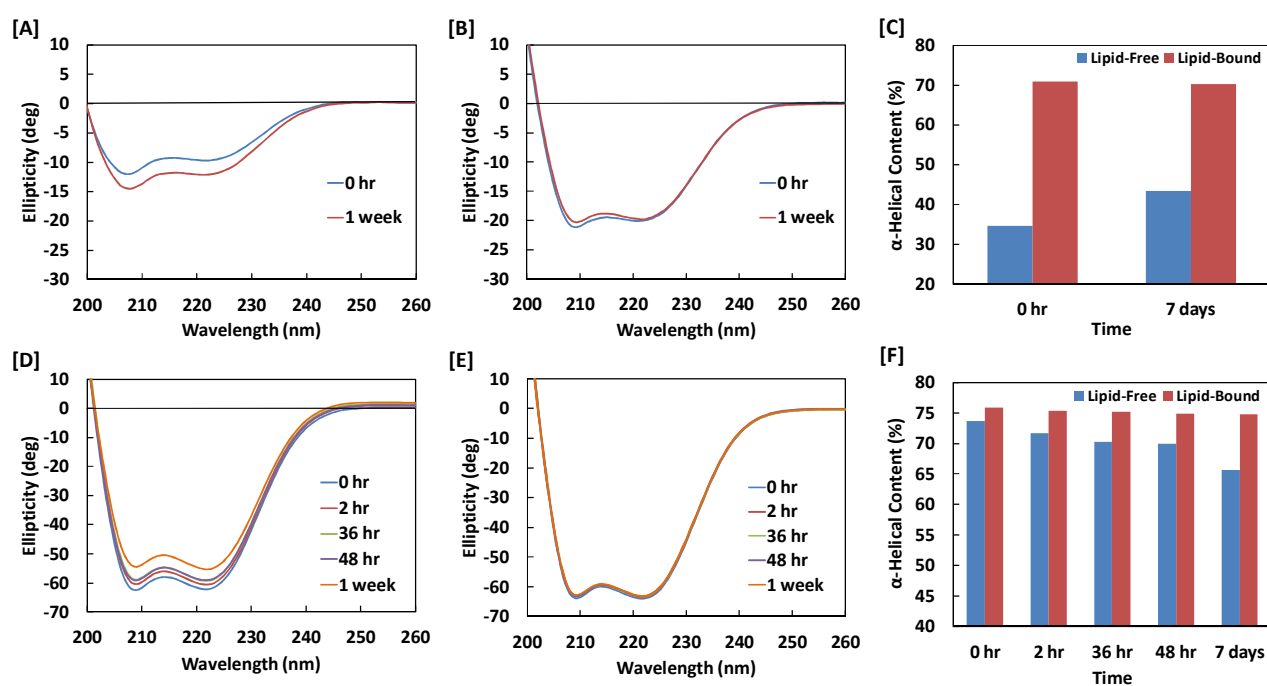


Figure 6: Circular dichroism spectra of [A] lipid-free MSP in solution and [B] lipid-bound MSP (NLPs) in solution, and [C] corresponding solution alpha-helix content determined from 222 nm ellipticity. Circular dichroism spectra of [D] lipid-free MSP in silica gel and [E] lipid-bound MSP (NLPs) in silica gel, with [F] corresponding gel alpha-helix content.

1
2
3 For all CD spectra in Fig. 6, two peaks characteristic of substantial alpha-helical content were
4 evident (located at 208 nm and 222 nm³⁴). The actual alpha-helical content was estimated from
5 the 222 nm peak using equations 3 and 4, as other secondary structural elements have little
6 contribution to this region of a protein spectrum.³⁵ In Fig. 6C, the alpha-helical content in buffer
7 solution was shown to remain at 70% for lipid-bound MSP and increase from 35% to 43% for
8 lipid-free MSP over the course of a week. In Fig. 6F, the alpha-helical content in silica gel was
9 shown to remain constant at 75% for lipid-bound MSP and decrease from 73% to 65% for lipid-
10 free MSP over the course of a week.
11
12
13
14
15
16
17
18
19
20
21

22 DISCUSSION

23
24 **Liposome and NLP Phase Behavior.** Liposomes can contain tens to hundreds of thousands of
25 lipids per structure and have cooperativity units that have been estimated to include up to 1700
26 lipid molecules.³⁶ Having fewer lipids per structure, NLPs are not capable of forming
27 cooperative units as large as those present in liposomes. The NLPs used in this work contained
28 roughly 375 lipids per disc. In addition, a fraction of the lipids, located in a two-lipid-thick belt
29 along the scaffold protein boundary, undergo a concomitant loss of cooperativity after NLP
30 formation.³⁷⁻³⁸ Therefore, in solution, NLPs inherently have a lower cooperativity index than
31 liposomes as we have observed here. The presence of scaffold proteins has also been shown to
32 elevate the phase transition temperature in solution, as observed here, for a given lipid
33 incorporated into NLPs compared to when incorporated into liposomes due to an increase in
34 lateral pressure from the protein-lipid interactions.³⁷
35
36
37
38
39
40
41
42
43
44
45
46
47
48
49

50 Upon entrapment in the silica gel, cooperativity of the NLP phase transition decreased slightly
51 (93% \pm 10% of solution value) while cooperativity of the liposomes decreased significantly
52 (12% \pm 3% of solution value). This leads us to believe that the liposomes are undergoing
53
54
55
56
57
58
59
60

1
2
3 significant structural changes upon entrapment, while the NLPs are not. A significant reduction
4
5 in size of liposomes has been shown to result in lowered cooperativity.³⁹ The rupturing of
6
7 liposomes and formation of smaller lipid aggregates or bicellar structures could reasonably
8
9 explain this observed behavior and has previously been observed in other works where
10
11 liposomes were entrapped in silica gel.²¹⁻²² Moreover, only a slight reduction in cooperativity
12
13 and elevation in phase transition temperature (compared to liposomes) for NLPs observed over
14
15 the course of 5-6 weeks could indicate that they are not undergoing significant alterations in their
16
17 size and structure after entrapment.
18
19
20

21
22 Upon silica gel entrapment, there was an observed elevation in phase transition temperature for
23
24 NLPs and liposomes, which is consistent with previous work where elevated phase transitions
25
26 for entrapped liposomes were observed due to speculated excluded volume effects.²¹ This is
27
28 analogous to effects observed in work with thermal unfolding of proteins in silica gel where a
29
30 higher free energy (thus higher unfolding temperature) was imposed upon entrapped, folded
31
32 proteins due to decreased volume available for the unfolded form.⁴⁰⁻⁴¹ Since the lipid tails
33
34 become less dense when undergoing a gel phase to liquid crystalline transition,⁴² it is reasonable
35
36 to believe the excluded volume effect can be involved. The observed decreased in anisotropy
37
38 range is due either to a change in the packing and motion of the lipid tails in each phase or
39
40 release of a portion of the DPH into the pores of the silica gel (See Supporting Information).
41
42 Nonetheless, a decrease in the anisotropy range does not have significant effect on the regressed
43
44 values for the cooperativity index or phase transition temperature (See Fig. S1).
45
46
47
48
49

50
51 We speculate that the minor (approximately 20%) reduction in cooperativity over weeks for
52
53 entrapped NLPs could be related to the known phenomenon of silica gel shrinkage over time.^{20,}
54

55
56 ⁴³ Since phospholipid headgroups are known to interact strongly with silica surfaces,²³ changes
57
58
59
60

1
2
3 in the geometry and size of pores could directly impact adsorbed NLPs. A decrease in size of
4 lipid structure is correlated to a decrease in cooperativity and could rationalize this observation;
5
6 however, the possibility of aggregation is not ruled out. A decrease in silica gel size corresponds
7
8 to a decrease in porosity, which would enhance the excluded volume effect, explaining our
9
10 observed increase in phase transition temperature over weeks for NLPs. Further work in
11
12 analyzing different silane precursors and monolith shrinkage effects on lipid structures would be
13
14 required to validate this hypothesis. Overall, these results make it very plausible that the silica
15
16 sol-gel-entrapped NLPs, unlike liposomes, maintain a structure resembling their solution
17
18 counterparts for weeks at a time.
19

20
21
22 **Methanol Effects on NLP Phase Behavior.** Due to the presence of residual methanol in the
23
24 silica gels (~5 v/v%), the effect of methanol on anisotropy values and phase behavior for NLPs
25
26 and liposomes in solution was examined. The trend in decreasing anisotropy and minimum T_m
27
28 values for NLPs and liposomes as the methanol concentration was increased is consistent with
29
30 previous fluorescence anisotropy studies involving short-chain alcohols,⁴⁴ as well as similar
31
32 studies in which lipid absorbance at 400 nm was utilized.⁴⁵⁻⁴⁶ Short-chained alcohols increase the
33
34 area per molecule of the lipid bilayer⁴⁷⁻⁴⁸ and induce the interdigitated phase,¹⁸ thus the DPH
35
36 probe is allowed to more freely rotate, lowering the anisotropy value. The minimum in the T_m
37
38 value is reported to correspond to the completion of the interdigitation transition.⁴⁵⁻⁴⁶ The
39
40 elevation in methanol concentration required to fully interdigitate NLPs could indicate that they
41
42 have a slightly higher resistance to bilayer interdigitation. The presence of the scaffold proteins
43
44 could perhaps prolong the bilayer structure in elevated methanol concentrations due to direct
45
46 interactions with the lipid tails, making it more difficult for them to interlace. The use of TMOS
47
48 instead of the popular precursor TEOS (tetraethylorthosilicate) is favorable due to its liberation
49
50
51
52
53
54
55
56
57
58
59
60

1
2
3 of methanol, which requires exponentially higher concentrations than ethanol to significantly
4 modulate lipid bilayer behavior.⁴⁸ We found that in the vicinity of 5 v/v% methanol, anisotropy
5 and T_m values for NLPs and liposomes was minimally changed. Therefore, the more significant
6 changes in these values for silica sol-gel-entrapped NLPs and liposomes were not caused by the
7 presence of methanol.
8
9

10 While the liposomes display a decrease in the cooperativity index, cooperativity increases for
11 NLPs with increasing methanol concentration. The interdigitated phase of bilayers tends to have
12 a lower phase transition temperature than the gel phase,^{18, 45-46} thus the decrease in the
13 cooperativity that is observed is potentially the result of coexistence between the gel and
14 interdigitated phases. This coexistence would result in the transition appearing broader, as the
15 phase transition equation used (Equation 2) only accounts for one inflection point. However, at
16 5 v/v% methanol, the cooperativity of the phase transition is only decreased by approximately
17 10% in comparison to 90% decrease observed for liposomes entrapped in silica gel. In the case
18 of the NLPs, the measured increase in aggregate size in methanol solutions would account for
19 larger cooperative units, which would directly increase the cooperativity index. The appearance
20 of the opposite trend, i.e. slightly decreasing cooperativity, for silica gel-entrapped NLPs
21 illustrates that the methanol concentration is below the threshold necessary for aggregate growth.
22
23
24
25
26
27
28
29
30
31
32
33
34
35
36
37
38
39
40
41
42

43 By removing most of the methanol through rotary evaporation in silica sol-gel-entrapped NLPs,
44 we have avoided significant changes in anisotropy and T_m caused by methanol. If we did not use
45 rotary evaporation, the solution methanol concentration was roughly 24 v/v% with
46 accompanying decreased anisotropy and T_m values, which were consistent in magnitude with
47 what was observed in solution experiments. However, the increase in cooperativity was minimal
48 compared to that observed in solution. The size of the pores (5-50 nm) could perhaps limit the
49
50
51
52
53
54
55
56
57
58
59
60

1
2
3 NLPs from aggregating or remodeling into larger lipid structures that would have cooperative
4
5 units comparable to those in solution.
6
7

8 **Protein Conformational Changes in NLPs.** The presence of alpha-helical secondary structure
9
10 is essential for NLP formation and protein-lipid binding.⁴⁹ We found that the alpha-helical
11
12 content of the scaffold protein MSP is significantly higher in its lipid-bound NLP-associated
13
14 state (70%), versus a lipid-free state (35%-43%) in solution. This magnitude of difference is
15
16 consistent with previous works that examined alpha helical content in very similar scaffold
17
18 proteins, such as MSP1D1⁵⁰ and Apolipoprotein A-I.^{49, 51-52} For Apolipoprotein A-I, this is due to
19
20 4 of the 10 helical regions forming a bundle in the lipid-free state, while the other 6 helical
21
22 regions, along with the globular region, fold in a variety of different conformations having
23
24 relatively higher random coil content.⁵³ It is reasonable to believe that similar behavior is
25
26 involved for MSP, as it is derived directly from Apolipoprotein A-I. Once entrapped in silica gel
27
28 the alpha-helical content of MSP in NLP samples increased slightly to 75%. Interestingly,
29
30 entrapped MSP in its lipid-free state adopted a significantly higher alpha-helical content than in
31
32 solution, increasing to 73%. These results are consistent with previous discoveries of the
33
34 biocompatible environment of silica sol-gels for water-soluble proteins which are often stabilized
35
36 against denaturation and aggregation in silica sol-gels. The stabilization effect has been
37
38 attributed to the ability of the sol-gel matrix to restrict conformational flexibility, diffusional
39
40 motion, and promote structural rigidity in the water environment.⁵⁴⁻⁵⁵ The confinement from the
41
42 pores of the silica gel could rationalize the observed increase in alpha-helical content for MSP
43
44 upon entrapment; an estimated radius of gyration of 3 nm for randomly structured MSP in
45
46 solution (See Supporting Information) is on the same order of magnitude as the pore size. This
47
48 could potentially cause MSP to adopt an alternative conformation that consists of higher alpha-
49
50
51
52
53
54
55
56
57
58
59
60

1
2
3 helical content. The decrease of alpha-helical content over the course of a week (73% - 65%) for
4 lipid-free MSP in silica gel in comparison to the steady alpha-helical content of 75% for lipid-
5 bound MSP could indicate that the silica gel promotes lipid association of MSP, thereby
6 maintaining the higher helical conformation of this state.^{49, 56} However, the absence of lipids
7 does not allow MSP to maintain a constant conformation.
8
9

15 CONCLUSIONS

17 We have demonstrated that Nanolipoprotein Particles (NLPs) are more compatible with the
18 nano-scale environment of the silica gel pores in comparison to liposomes. Direct measurement
19 of size of soft matter inside of mesoporous silica is difficult to obtain, thus we utilized
20 biophysical characterization in the form of fluorescence anisotropy and circular dichroism
21 spectroscopy to directly investigate lipid phase behavior and scaffold protein secondary
22 structure, as well as indirectly correlate this behavior to aggregate size. Fluorescence anisotropy,
23 which is then used to analyze cooperativity and temperature of the main phase transition,
24 revealed that NLPs entrapped in silica gel exhibit phase behavior with a stronger resemblance to
25 their solution counterparts than liposomes. In particular, cooperativity indices indicate that
26 entrapment in silica gel causes immediate large scale changes in lipid aggregation state of
27 liposomes toward smaller cooperative units, and only minor changes for NLPs over weeks of
28 time. These large scale changes in liposomes have been linked in the past to liposome rupture
29 and denaturation of integral membrane proteins. By investigating these same properties for
30 liposomes and NLPs in methanol solutions, we find that the small amount of methanol remaining
31 after evaporative removal is not sufficient to cause observed changes in these properties upon
32 sol-gel entrapment. However, if we did not remove the methanol we found that entrapped NLPs
33 displayed shifts in anisotropy and phase transition temperature that were consistent with large
34
35
36
37
38
39
40
41
42
43
44
45
46
47
48
49
50
51
52
53
54
55
56
57
58
59
60

1
2
3 fractions of methanol but that the cooperativity was relatively maintained, which we attribute to
4
5 limitations in the growth of the NLPs by confinement in the nanoporous environment of the
6
7 silica gel. Upon further investigation of conformational changes, circular dichroism revealed
8
9 that the scaffold protein of the entrapped NLPs maintained a consistent alpha-helical content
10
11 necessary for its structural function of belting the phospholipids. This is consistent with the
12
13 known biocompatibility and structure promotion of silica gels for water soluble proteins. Future
14
15 work would entail the incorporation of integral membrane proteins inside of NLPs and
16
17 analysis/quantification of their activity retention upon sol-gel derived entrapment via protein
18
19 specific assays.
20
21
22
23

24 **ACKNOWLEDGMENTS**

25
26
27 The project described was supported by Grant Number T32-GM008799 from NIGMS-NIH. Its
28
29 contents are solely the responsibility of the authors and do not necessarily represent the official
30
31 views of the NIGMS or NIH.
32
33

34 **SUPPORTING INFORMATION**

35
36 Detailed methods, calculations, and figures. This material is available free of charge via the
37
38 Internet at <http://pubs.acs.org>.
39
40

41 **REFERENCES**

- 42
43
44 (1) Avnir, D.; Coradin, T.; Lev, O.; Livage, J. Recent Bio-Applications of Sol–Gel Materials. *J.*
45
46 *Mater. Chem.* **2006**, *16* (11), 1013-1030.
47
48
49 (2) Nassif, N.; Livage, J. From Diatoms to Silica-Based Biohybrids. *Chem. Soc. Rev.* **2011**, *40*
50
51 (2), 849-59.
52
53
54 (3) Ruiz-Hitzky, E.; Ariga, K.; Lvov, Y. *Bio-Inorganic Hybrid Nanomaterials: Strategies,*
55
56 *Syntheses, Characterization and Applications*; WILEY-VCH Weinheim, Germany, 2008.
57
58
59
60

- 1
2
3
4
5
6
7
8
9
10
11
12
13
14
15
16
17
18
19
20
21
22
23
24
25
26
27
28
29
30
31
32
33
34
35
36
37
38
39
40
41
42
43
44
45
46
47
48
49
50
51
52
53
54
55
56
57
58
59
60
- (4) Gill, I. Bio-Doped Nanocomposite Polymers: Sol-Gel Bioencapsulates. *Chem. Mater.* **2001**, *13* (10), 3404-3421.
 - (5) Brennan, J. D. Biofriendly Sol-Gel Processing for Entrapment of Soluble and Membrane-Bound Proteins: Toward Novel Solid-Phase Assays for High-Throughput Screening. *Acc. Chem. Res.* **2007**, *40* (9), 827-835.
 - (6) Kato, M.; Sakai-Kato, K.; Toyo'oka, T. Silica Sol-Gel Monolithic Materials and Their Use in a Variety of Applications. *J. Sep. Sci.* **2005**, *1893-1908*.
 - (7) Monton, M. R. N.; Forsberg, E. M.; Brennan, J. D. Tailoring Sol-Gel Derived Silica Materials for Optical Biosensing. *Chem. Mater.* **2012**, *24* (5), 796-811.
 - (8) Avdulov, N. A.; Chochina, S. V.; Draski, L. J.; Deitrich, R. A.; Wood, W. G. Chronic Ethanol Consumption Alters Effects of Ethanol in Vitro on Brain Membrane Structure of High Alcohol Sensitivity and Low Alcohol Sensitivity Rats *Alcohol.: Clin. Exp. Res.* **1995**, *19* (4), 886-891.
 - (9) Lu, J. Z.; Huang, F.; Chen, J. W. The Behaviors of Ca²⁺ ATPase Embedded in Interdigitated Bilayer. *J. Biochem.* **1999**, *126* (2), 302-306.
 - (10) Lucero, P.; Penalver, E.; Monero, E.; Lagunas, R. Moderate Concentrations of Ethanol Inhibit Endocytosis of the Yeast Maltose Transporter. *Appl. Environ. Microbiol.* **1997**, *63* (10), 3831-3836.
 - (11) Mitchell, D. C.; Lawrence, J. T. R.; Litman, B. J. Primary Alcohols Modulate the Activation of the G Protein-Coupled Receptor Rhodopsin by a Lipid-Mediated Mechanism. *J. Biol. Chem.* **1996**, *271* (32), 19033-19036.

- 1
2
3
4 (12) Flora, K. K.; Brennan, J. D. Effect of Matrix Aging on the Behaviour of Human Serum
5 Albumin Entrapped in a Tetraethylorthosilicate-Derived Glass. *Chem. Mater.* **2001**, *13* (11),
6 4170-4179.
7
8
9
10 (13) Baker, G. A.; Jordan, J. D.; Bright, F. V. Effects of Poly(Ethylene Glycol) Doping on the
11 Behavior of Pyrene, Rhodamine 6g, and Acrylodan-Labeled Bovine Serum Albumin
12 Sequestered within Tetramethylorthosilane-Derived Sol-Gel-Processed Composites. *J. Sol-*
13 *Gel Sci. Technol.* **1998**, *11* (1), 43-54.
14
15
16
17 (14) Gottfried, D. S.; Kagan, A.; Hoffman, B. M.; Friedman, J. M. Impeded Rotation of a Protein
18 in a Sol-Gel Matrix. *J. Phys. Chem.* **1999**, *103* (14), 2803-2807.
19
20
21
22 (15) Shen, C.; Kostic, N. M. Kinetics of Photoinduced Electron Transfer Reactions within Sol-
23 Gel Silica Glass Doped with Zinc Cytochrome C. *J. Am. Chem. Soc.* **1997**, *119* (6), 1304-
24 1312.
25
26
27
28 (16) Eggers, D. K.; Valentine, J. S. Crowding and Hydration Effects on Protein Conformation: A
29 Study with Sol-Gel Encapsulated Proteins. *J. Mol. Biol.* **2001**, *314* (4), 922-922.
30
31
32
33 (17) Brennan, J. D.; Benjamin, D.; Dibattista, E.; Gulcev, M. D. Using Sugar and Amino Acid
34 Additives to Stabilize Enzymes within Sol-Gel Derived Silica. *Chem. Mater.* **2003**, *15* (3),
35 737-745.
36
37
38
39 (18) Slater, J. L.; Huang, C. Interdigitated Bilayer Membranes. *Prog. Lipid Res.* **1988**, *27* (4),
40 325-359.
41
42
43
44 (19) Chen, Y.; Zhang, Z.; Sui, X. H.; Brennan, J. D. Reduced Shrinkage of Sol-Gel Derived
45 Silicas Using Sugar-Based Silsequioxane Precursors. *J. Mater. Chem.* **2005**, *15* (30), 3132-
46 3141.
47
48
49
50
51
52
53
54
55
56
57
58
59
60

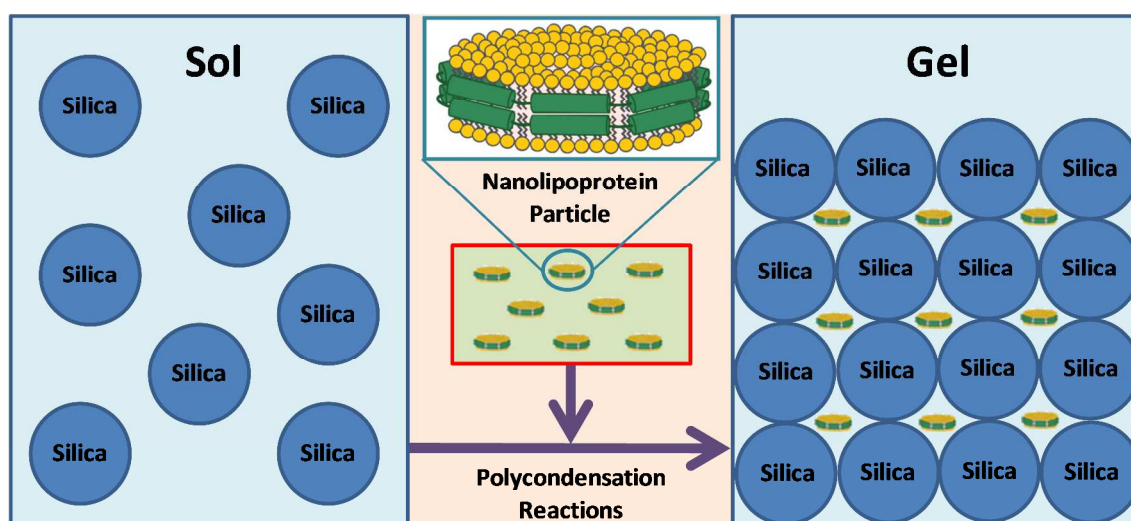
- 1
2
3
4 (20) Brook, M. A.; Chen, Y.; Guo, K.; Zhang, Z.; Brennan, J. D. Sugar-Modified Silanes:
5
6 Precursors for Silica Monoliths. *J. Mater. Chem.* **2004**, *14* (9), 1469-1479.
7
8 (21) Besanger, T.; Zhang, Y.; Brennan, J. D. Characterization of Fluorescent Phospholipid
9
10 Liposomes Entrapped in Sol-Gel Derived Silica. *J. Phys. Chem. B* **2002**, *106* (41), 10535-
11
12 10542.
13
14 (22) Halder, A.; Sen, S.; Burman, A. D.; Patra, A.; Bhattacharyya, K. Solvation Dynamics of
15
16 Dimyristoyl-Phosphatidylcholine Entrapped inside a Sol-Gel Matrix. *J. Phys. Chem. B*
17
18 **2004**, *108* (7), 2309-2312.
19
20 (23) Reimhault, E.; Hook, F.; Kasemo, B. Intact Vesicle Adsorption and Supported
21
22 Biomembrane Formation from Vesicles in Solution: Influence of Surface Chemistry,
23
24 Vesicle Size, Temperature, and Osmotic Pressure. *Langmuir* **2003**, *19* (5), 1681-1691.
25
26 (24) Reimhault, E.; Zach, M.; Hook, F.; Kasemo, B. A Multitechnique Study of Liposome
27
28 Adsorption on Au and Lipid Bilayer Formation on SiO₂. *Langmuir* **2006**, *22* (7), 3313-3319.
29
30 (25) Tero, R.; Takizawa, M.; Li, Y.; Yamazaki, M.; Urisu, T. Lipid Membrane Formation by
31
32 Vesicle Fusion on Silicon Dioxide Surfaces Modified with Alkyl Self-Assembled
33
34 Monolayer Islands. *Langmuir* **2004**, *20* (18), 7526-7531.
35
36 (26) Jing, Y.; Trefna, H.; Persson, M.; Kasemo, B.; Svedhem, S. Formation of Supported Lipid
37
38 Bilayers on Silica: Relation to Lipid Phase Transition Temperature and Liposome Size. *Soft*
39
40 *Matter* **2014**, *10* (1), 187-195.
41
42 (27) Ferrer, M.; Del Monte, F.; Levy, D. A Novel and Simple Alcohol Free Sol Gel Route for
43
44 Encapsulation of Labile Proteins. *Chem. Mater.* **2002**, *14* (9), 3619-3621.
45
46
47
48
49
50
51
52
53
54
55
56
57
58
59
60

- 1
2
3 (28) Luo, T. J.; Soong, R.; Lan, E.; Dunn, B.; Montemagno, C. Photo-Induced Proton Gradients
4 and ATP Biosynthesis Produced by Vesicles Encapsulated in a Silica Matrix. *Nat. Mater.*
5
6
7
8 **2005**, *4* (3), 220-224.
9
- 10 (29) Besanger, T.; Easwaramoorthy, B.; Brennan, J. D. Entrapment of Highly Active Membrane
11 Bound Receptors in Macroporous Silica. *Anal. Chem.* **2004**, *76* (21), 6470-6475.
12
13
- 14 (30) Bricarello, D. A.; Smilowitz, J. T.; Zivkovic, A. M.; German, J. B.; Parikh, A. N.
15 Reconstituted Lipoprotein: A Versatile Class of Biologically-Inspired Nanostructures. *ACS*
16
17
18
19
20
21 *Nano* **2011**, *5* (1), 42-57.
22
- 23 (31) Lakowicz, J. *Principles of Fluorescence Spectroscopy* Springer: New York, 2006.
24
- 25 (32) Nelson, S. C.; Neeley, S. K.; Melonakos, E. D.; Bell, J. D.; Busath, D. D. Fluorescence
26 Anisotropy of Diphenylhexatriene and its Cationic Trimethylamino Derivative in Liquid
27 Dipalmitoylphosphatidylcholine Liposomes: Opposing Responses to Isoflurane. *BMC*
28
29
30
31
32
33 *Biophys.* **2012**, *5* (1), 5.
34
- 35 (33) Morrow, J. A.; Segall, M. L.; Lund-Katz, S.; Phillips, M. C.; Knapp, M.; Rupp, B.;
36 Weisgraber, K. H. Differences in Stability among the Human Apolipoprotein E Isoforms
37 Determined by the Amino-Terminal Domain. *Biochemistry* **2000**, *39* (8), 11657-11666.
38
39
- 40 (34) Kelly, S. M.; Jess, T. J. How to Study Proteins by Circular Dichroism. *Biochim. Biophys.*
41
42
43
44
45 *Acta* **2005**, *1751* (2), 119-139.
46
- 47 (35) Hirst, J. D.; Brooks, C. L. Helicity, Circular Dichroism and Molecular Dynamics of
48 Proteins. *J. Mol. Biol.* **1994**, *243* (2), 173-178.
49
- 50 (36) Knoll, W. Calorimetric Investigations of Lipid Phase Transitions. I. The Width of
51 Transition. *Thermochim. Acta* **1984**, *77* (1), 35-47.
52
53
54
55
56
57
58
59
60

- 1
2
3
4 (37) Denisov, I. G.; McLean, M. A.; Shaw, A. W.; Grinkova, Y. V.; Sligar, S. G. Thermotropic
5
6 Phase Transition in Soluble Nanoscale Lipid Bilayers. *J. Phys. Chem. B* **2005**, *109* (32),
7
8 15580-15588.
9
- 10 (38) Shaw, A. W.; McLean, M. A.; Sligar, S. G. Phospholipid Phase Transitions in
11
12 Homogeneous Nanometer Scale Bilayer Discs. *FEBS Lett.* **2004**, *556* (1), 260-264.
13
14
- 15 (39) Marsh, D.; Watts, A.; Knowles, P. F. Cooperativity of the Phase Transition in Single- and
16
17 Multibilayer Lipid Vesicles. *Biochim. Biophys. Acta* **1977**, *465* (3), 500-514.
18
19
- 20 (40) Eggers, D. K.; Valentine, J. S. Molecular Confinement Influences Protein Structure and
21
22 Enhances Thermal Protein Stability *Protein Sci.* **2001**, *10* (2), 250-261.
23
24
- 25 (41) Zhou, H.; Dill, K. Stabilization of Proteins in Confined Spaces. *Biochemistry* **2001**, *40* (38),
26
27 11289-11293.
28
- 29 (42) Xie, A. F.; Yamada, R.; Gewirth, A. A.; Granick, S. Materials Science of the Gel to Fluid
30
31 Phase Transition in a Supported Phospholipid Bilayer. *Phys. Rev. Lett.* **2002**, *89* (24),
32
33 246103.
34
35
- 36 (43) Brinker, C. J.; Scherer, G. W. *Sol-Gel Science: The Physics and Chemistry of Sol-Gel*
37
38 *Processing*; Academic Press: San Diego, 1990.
39
40
- 41 (44) Kim, Y. H.; Higuchi, W. I.; Herron, J. N.; Abraham, W. Fluorescence Anisotropy Studies
42
43 on the Interaction of the Short Chain n-Alkanols with Stratum Corneum Lipid Liposomes
44
45 (SCLL) and Distearoylphosphatidylcholine (DSPC)/Distearoylphosphatidic Acid (DSPA)
46
47 Liposomes. *Biochemica et Biophysica Acta (BBA)- Biomembranes* **1993**, *1148* (1), 139-151.
48
49
- 50 (45) Rowe, E. S. Thermodynamic Reversibility of Phase Transitions. Specific Effects of
51
52 Alcohols on Phosphatidylcholines. *Biochemica et Biophysica Acta (BBA)- Biomembranes*
53
54 **1985**, *813* (2), 321-330.
55
56
57
58
59
60

- 1
2
3 (46) Koynova, R.; Caffrey, M. Phases and Phase Transitions of the Phosphatidylcholines.
4
5 *Biochimica et Biophysica Acta (BBA)- Reviews on Biomembranes* **1998**, *1376* (1), 91-145.
6
7
8 (47) Ly, H. V.; Block, D. E.; Longo, M. L. Interfacial Tension Effect of Ethanol on Lipid Bilayer
9
10 Rigidity, Stability, and Area/Molecule: A Micropipet Aspiration Approach. *Langmuir*
11
12 **2002**, *18* (23), 8988.
13
14
15 (48) Ly, H. V.; Longo, M. L. The Influence of Short-Chain Alcohols on Interfacial Tension,
16
17 Mechanical Properties, Area/Molecule, and Permeability of Fluid Lipid Bilayers. *Biophys.*
18
19 *J.l* **2004**, *87* (2), 1013-33.
20
21
22 (49) Saito, H.; Dhanasekaran, P.; Nguyen, D.; Deridder, E.; Holvoet, P.; Lund-Katz, S.; Phillips,
23
24 M. C. A-Helix Formation Is Required for High Affinity Binding of Human Apolipoprotein
25
26 A-I to Lipids. *J. Biol. Chem.* **2004**, *279* (20), 20974-20981.
27
28
29 (50) Morgan, C. R.; Hebling, C. M.; Rand, K. D.; Stafford, D. W.; Jorgenson, J. W.; Engen, J. R.
30
31 Conformational Transitions in the Membrane Scaffold Protein of Phospholipid Bilayer
32
33 Nanodiscs. *Mol. Cell. Proteomics* **2011**, *10* (9), M111-010876.
34
35
36 (51) Alexander, E. T.; Tanaka, M.; Kono, M.; Saito, H.; Rader, D. J.; Phillips, M. C. Structural
37
38 and Functional Consequences of the Milano Mutation (R173c) in Human Apolipoprotein
39
40 AI. *J. Lipid Res.* **2009**, *50* (7), 1409-1419.
41
42
43 (52) Petrova, J.; Dalla-Riva, J.; Mörgelin, M.; Lindahl, M.; Krupinska, E.; Stenkula, K. G.;
44
45 Voss, J. C.; Lagerstedt, J. O. Secondary Structure Changes in ApoA-I Milano (R173C) Are
46
47 Not Accompanied by a Decrease in Protein Stability or Solubility. *PloS one* **2014**, *9* (4),
48
49 e96150.
50
51
52
53
54
55
56
57
58
59
60

- 1
2
3
4
5
6
7
8
9
10
11
12
13
14
15
16
17
18
19
20
21
22
23
24
25
26
27
28
29
30
31
32
- (53) Pollard, R. D.; Fulp, B.; Samuel, M. P.; Sorci-Thomas, M. G.; Thomas, M. J. The Conformation of Lipid-Free Human Apolipoprotein A-I in Solution. *Biochemistry* **2013**, *52* (52), 9470-81.
- (54) Zheng, L.; Brennan, J. D. Measurement of Intrinsic Fluorescence to Probe the Conformational Flexibility and Thermodynamic Stability of a Single Tryptophan Protein Entrapped in a Sol-Gel Derived Glass Matrix. *Analyst* **1998**, *123* (8), 1735-1744.
- (55) Das, T. K.; Khan, I.; Rousseau, D. L.; Friedman, J. M. Preservation of the Native Structure in Myoglobin at Low pH by Sol-Gel Encapsulation. *J. Am. Chem. Soc.* **1998**, *120* (39), 10268-10269.
- (56) Nolte, R. T.; Atkinson, D. Conformational Analysis of Apolipoprotein a-I and E-3 Based on Primary Sequence and Circular Dichroism. *Biophys. J.* **1992**, *63* (5), 1221-1239.



50
51
52
53
54
55
56
57
58
59
60

Abstract Graphic